Droplet Microfluidics for the Production of Microparticles and Nanoparticles

Jianmei Wang [1,2], Yan Li [2], Xueying Wang [2], Jianchun Wang [2], Hanmei Tian [2], Pei Zhao [2], Ye Tian [3], Yeming Gu [4], Liqiu Wang [2,3,*] and Chengyang Wang [1,*]

[1]   School of Chemical Engineering and Technology, Tianjin University, Tianjin 300072, China; wangjm@sderi.cn
[2]   Energy Research Institute, Shandong Academy of Sciences, Jinan 250014, China; liyan@sderi.cn (Y.L.); wangxy@sderi.cn (X.W.); wangjc@sderi.cn (J.W.); tianhm@sderi.cn (H.T.); zhaop@sderi.cn (P.Z.)
[3]   Department of Mechanical Engineering, The University of Hong Kong, Hong Kong, China; tianye@hku.hk
[4]   Shandong Shengli Co., Ltd., Jinan 250101, China; perfectgu@126.com
*   Correspondence: lqwang@hku.hk (L.W.); cywang@tju.edu.cn (C.W.); Tel.: +86-531-8872-8326 (L.W.); +86-22-2789-0481 (C.W.)

Abstract: Droplet microfluidics technology is recently a highly interesting platform in material fabrication. Droplets can precisely monitor and control entire material fabrication processes and are superior to conventional bulk techniques. Droplet production is controlled by regulating the channel geometry and flow rates of each fluid. The micro-scale size of droplets results in rapid heat and mass-transfer rates. When used as templates, droplets can be used to develop reproducible and scalable microparticles with tailored sizes, shapes and morphologies, which are difficult to obtain using traditional bulk methods. This technology can revolutionize material processing and application platforms. Generally, microparticle preparation methods involve three steps: (1) the formation of micro-droplets using a microfluidics generator; (2) shaping the droplets in micro-channels; and (3) solidifying the droplets to form microparticles. This review discusses the production of microparticles produced by droplet microfluidics according to their morphological categories, which generally determine their physicochemical properties and applications.

Keywords: microfluidics; microparticles; nanoparticles; monodisperse; emulsion; droplet microfluidics

1. Introduction

Monodisperse microparticles and nanoparticles with uniform sizes and morphologies are used in bio-pharmaceuticals [1,2], drug delivery applications [3,4], electro/optic devices [5,6] and catalysis [7–9] because of their unique properties. Many efforts are made to produce uniform microparticles with custom sizes, shapes and morphologies using traditional methods, such as precipitation polymerization [10,11], emulsion polymerization [12,13], dispersion polymerization [14,15], SPG (Shirasu Porous Glass) membrane emulsification [16,17], and layer-by-layer assemblies [18]. However, these conventional emulsion droplet methods with bulk shearing forces are uncontrollable, and the resulting droplets, especially the non-spherical particles, are disparate in size and shape. Because of the interfacial tensions between the two phases, the emulsion droplets automatically shrink into spheres, making it difficult for traditional methods to prepare quality custom shaped particles. Moreover, traditional methods are complex, inflexible and expensive. Therefore, better methods are needed to produce monodisperse microparticles with tailored sizes, shapes and morphologies.

Droplet microfluidics techniques, including active and passive method are promising methods to generate monodisperse emulsions. The main difference between active and passive methods is based on the external forces. Active droplet generators are usually achieved by incorporating additional

forces into microfluidic systems, such as electrical [19], magnetic [20], pneumatic [21], acoustic [22] and thermal [23]. Co-flow [24,25], flow-focusing [26–28], T-junction [29,30], step emulsification [31] and microchannel terraces [32,33] are basic passive droplet generators. The active control offers more flexibility in manipulating droplet than passive droplet generation. However, the active methods suffer from difficulties in fabrication and miniaturization. In this review, we will mainly focus on the passive methods. These approaches operate in the laminar flow region and generate one drop at a time. The conditions are identical for each droplet as it breaks off [34,35], and the produced emulsions are uniform in size, structure and composition [36]. In addition, the microfluidic devices provide much more flexibility because only the device structures need to be changed to produce complex structure droplets, such as single-emulsions, double-emulsions and multi-emulsions [37,38].

The superior properties of droplet microfluidics are advantageous for precise microparticle manufacturing, especially when used as templates to prepare microparticles and nanoparticles with various morphologies. In general, highly monodisperse emulsified droplets form in a microfluidic device and are simultaneously used as a template, and then are solidified to form microparticles and nanoparticles by chemical, photochemical or physical methods [39]. This review discusses recent advances in microparticle and nanosphere fabrication with droplet microfluidics. Because a single emulsion can be a template for solid spheres, and double or multi-emulsions can be templates for core shells, Janus or other morphology spheres, we classified the emulsion droplets according to their structures, and focused on how the emulsion droplets evolved into various structures and morphologies, as shown in Figure 1. This review provides a general background to those new to droplet microfluidics.
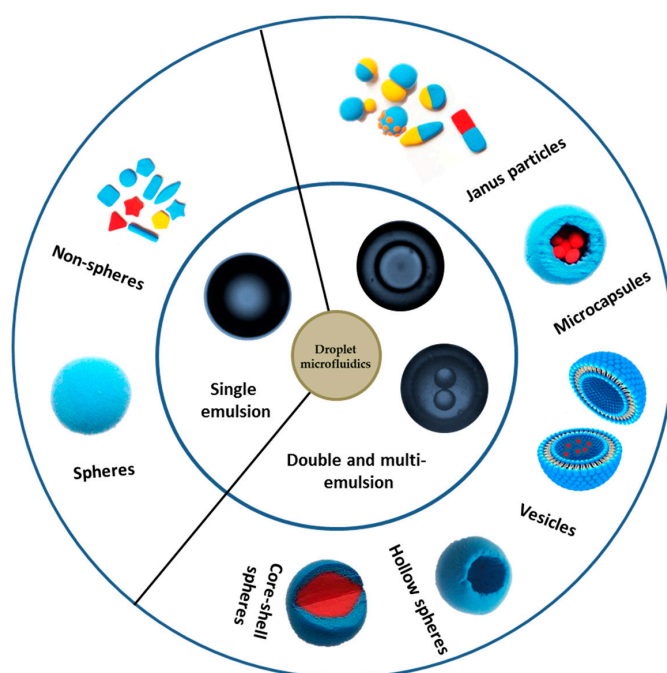
Figure 1. Summary of applications for microparticles and nanoparticles.

2. Microparticles and Nanoparticles with Single Emulsion Template

Single emulsions are droplets of one phase fluid dispersed in another immiscible phase fluid. The key step in forming monodisperse microparticles is to form monodisperse droplets with microfluidic devices. The most frequently used systems to generate monodisperse droplets are co-flow, cross-flow, and flow focusing, and the coefficient of variation (CV, defined as the ratio of standard deviation to the mean of the droplet radius) of droplets is usually less than 5% [40]. The size of the droplets generated from co-flow and cross-flow is often related to the dispersed channel dimension,

whereas flow-focusing structure is different from the above two types. In flow-focusing, the inner fluid is hydrodynamically flow focused by the outer fluid through the orifice, and it allows generating droplets with smaller size than that of the orifice. Based on this feature, we can use a larger orifice to make droplets for those fluids with suspended particles, to minimize the probability of clogging the orifice.

Chong et al. [41] and Zhu et al. [42] gave a very detailed summary on the active and passive droplet generation methods with microfluidic devices, in which they overviewed the different droplet generators and the characteristics and mechanisms of breakup modes of droplet generation. The five breaking modes in passive generation, which are squeezing, dripping, jetting, tip-streaming and tip-multi-breaking have their own unique characteristics, and can be applied to various fields, for example, to perform chemical and biochemical reactions where droplets used as microreactors [43,44] and to synthesis microparticles with droplets as templates [45–48]. In material science, this is a superior tool for engineering micromaterials and nanomaterials, we can change the component and the structure of the droplets to produce polymer particles, inorganic nanoparticles and metal particles [49]. In this section, we will discuss how single emulsions are used as templates for generating solid particles, including spherical and non-spherical particles with different materials.

2.1. Spherical Particles

2.1.1. Polymer Microspheres

Polymer microspheres are commonly used in pharmaceutical and medical applications. Polyvinyl alcohol (PVA), poly(lactic-co-glycolic acid) (PLGA), sodium alginate, polyethylene glycol (PEG) and gelatin microspheres have been successfully used as drug carriers [26,39,50–56]. Several methods, such as spray-drying, coacervation and emulsification, are used to prepare polymer microspheres. However, these conventional bulk procedures cannot be precisely controlled and result in polydispersed and irregular shapes, which limits their practical applications [57].

Xu et al. used flow-focusing geometry to generate PLGA droplets in PDMS devices [58]. They produced monodisperse particles with defined sizes ranging from 10 to 50 μm by simply tuning the flow rates of the continuous phase and the disperse phase. After loading bupivacaine (an amphiphilic drug), they found that the drug release kinetics of the monodisperse particles were different from those of the polydisperse particles produced by conventional methods. The monodisperse PLGA microparticles had significantly reduced burst releases and slower overall release rates than those of the polydisperse particles under the similar conditions.

Chu et al. used a glass capillary-based single emulsion device as shown in Figure 2 to make monodisperse Poly(Nisopropylacrylamide) (PNIPAm) microgels [46]. The spherical voids were introduced in a controlled manner into the microgels. They found that the microgels with voids would swell and shrink in response to temperature changes faster than those with voidless microgels. In addition, the response rates were finely tuned by changing the size and number of spherical voids inside the microgels.
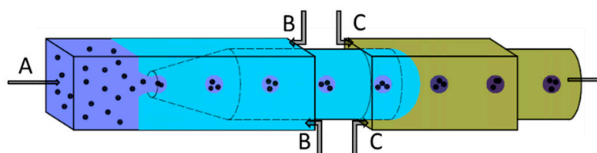
Figure 2. Schematic illustration of a capillary-based single emulsion device for fabricating monodisperse PNIPAm microgels. This device was used by Chu et al. [46]. **A** containing the monomer (N-isopropylacrylamide), a crosslinker (*N*,*N*′-methylene-bis-acrylamide), and a reaction initiator (ammonium persulfate) and solid polystyrene particles; **B** containing the kerosene and a surfactant; and **C** amphipathic reaction accelerator (*N*,*N*,*N*′,*N*′-tetramethyethylenediamine) dissolved in kerosene.

Seo et al. studied the emulsification of four kinds of monomer acrylates to synthesize polymer particles in a microfluidic flow-focusing device [59]. They detailed the effects of hydrodynamic conditions, channel geometry and micro-device materials on the size of the droplets. The selection of an appropriate material for the device was a vital stage in the generation of the droplets, and phase inversion occurred because of the higher affinity of the droplet phase for the material of the microfluidic device, such as glass, silicon, polydimethylsiloxane (PDMS) and polyurethane (PU). Though the channel surface could be modified by surfactants, the modified effect disappeared after several hours of emulsification. In addition, the rate of monomer polymerization with UV-light affected the quality of the sphere. Rapid polymerization caused enough heat to induce an explosion and a vacuum for low monomer-to-polymer conversion caused the sphere to collapse. Serra et al. produced polymer particles without surfactant or pretreatment in a co-flow device, and studied the effect of the viscosity of the continuous phase on the particle size [60]. They found high viscosity of the continuous phase could prevent the droplets from phase inversion and generate smaller particles for a given fluid flow rate. It could be of particular interest for the synthesis of particles with a functionalized surface.

Controlling the composition of the particles allows for a variety of functional properties. When dyes, semiconductor quantum dots, magnetic nanoparticles or liquid crystals are added to the particles, they have an optical, magnetic and actuation performance [61–65]. Carrying chemo-therapeutic or radio-therapeutic agents in the embolism microspheres greatly improves the treatment effects [66,67]. Magnetically guided drug carriers for medical imaging and therapeutic applications have been studied for decades and are currently ready for clinical trials [68,69]. These applications are available by adding another functional composition in the disperse phase to form stable droplet, and then by delivering the droplet into the microsphere.

2.1.2. Inorganic Microspheres

Monodisperse inorganic microspheres, including those composed of silica, carbon, and titanium, have received considerable attention for their potential applications in biomolecules, drug delivery [70,71], sensors [6] and catalysts [9]. The classical Stőber method is a general approach for the synthesis of silica spheres based on sol-gel chemistry. The synthesis involves the hydrolysis and condensation of silicon alkoxides in alcohol solvents with ammonia as the catalyst, and produces monodisperse silica spheres of predetermined sizes in the range 0.05–2 μm [72]. However, the particle sizes are not precisely reproducible with this method. Liu et al. extended this method to prepare monodisperse resorcinol-formaldehyde resin polymers (RFs) and carbon spheres, and the particle sizes of the RFs and carbon spheres were tuned from 200 nm to 1000 nm by varying the concentration of the reactant [73]. However, this method is not generally used to prepare other materials, especially when preparations require precise control over the particle sizes across wider ranges and shapes.

Lee et al. [47], Carroll and another researchers [74,75] reported a one-step method to manipulate ordered mesoporous silica (OMS) in a microfluidic device. This method combined a microfluidic emulsification technique and a rapid solvent diffusion induced self-assembly (DISA) technique. Monodisperse droplets were generated at the flow-focusing orifice and assembled into mesostructured silica/surfactant composite spheres within the microchannel, as shown in Figure 3. The sizes and the surface morphologies were easily controlled by changing the synthesis parameters, such as the geometry of the microfluidic channels, the flow rate of the precursor solution and oil, and the type of oil.
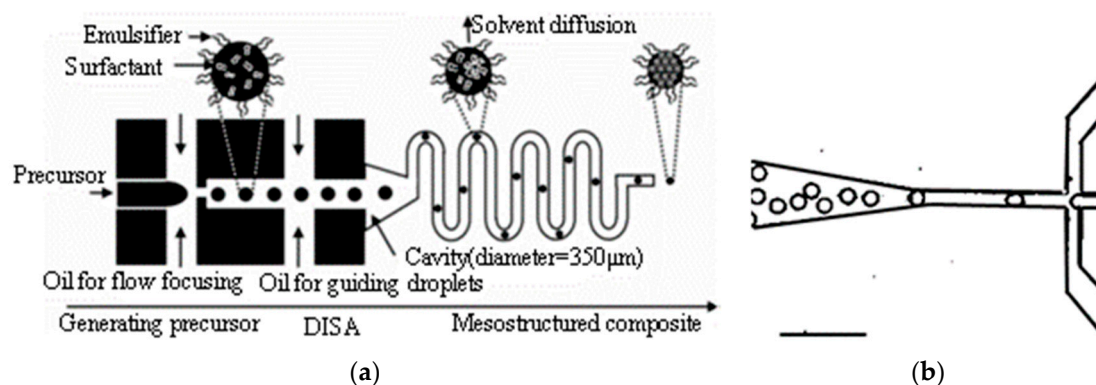
Figure 3. (**a**) Schematic illustration of the synthesis of OMS particles using microfluidic DISA used by Lee et al. [47]. Reproduced with permission from Lee, I., et al., *Advanced Functional Materials*; published by John Wiley and Sons, 2008. (**b**) Optical microscopy image of droplets of the silica precursor solution emulsified in a flow focusing microfluidic device in hexadecane from Carroll et al. [74]. The channel dimensions of the orifice are 25 μm in width and 30 μm in length. The scale bar is 100 μm. Reproduced with permission from Carrol, N.J., et al., *Langmuir*; published by American Chemical Society, 2008.

2.1.3. Noble Metal Nanospheres

Noble metal nanoparticles, such as gold, silver and platinum, are interesting materials because of their size and shape dependent properties [49,76–84]. However, the individual nanoparticles tend to coagulate and precipitate to lower the surface free energy. Therefore, these materials are difficult to use to obtain a desired size and size distribution.

The control of the crystal structure of the nanoparticles is another key issue in nanoparticle synthesis. Heat and mass control is very important to crystal growth, and the droplet microfluidics device provides a unique platform to precisely control heat and mass, which results from the fast heat and mass-transfer rates in the microchannel due to the short diffusion pathways induced by the small characteristic lengths of microfluidic device.

Gold nanoparticles have received considerable attention because of their broad range of applications. Recently, gold nanoparticles were synthesized from spherical gold nanoparticle seeds <4 nm in size in the microfluidic device [85]. Various shapes such as spheres, spheroids, rods and extended sharp-edged structures were obtained by tuning the concentrations of reagents and feed rates of the individual aqueous streams.

2.1.4. Semiconductor Nanospheres

Droplet microfluidics are commonly used in synthesizing nanoparticles at room temperature [86], but the pyrolytic synthesis of high quality semiconductor nanocrystals, such as CdSe, requires higher reaction temperatures of 200–350 °C, which renders this method impractical. The droplets and carrier fluids should be stable, non-interacting, non-volatile and immiscible from ambient to reaction temperatures, and the microfluidic reactor must have thermal and chemical stability [87].

Chan et al. used octadecene (ODE) as the solvent, long-chained perfluorinated polyethers (PFPEs) with high-boiling points as the continuous fluids and glass as the microreactor material. All fluids and device materials were stable at the reaction temperature [87]. However, this system had a low interfacial tension (γ) (5–25 mN/m) and a high viscosity (μ) (>100 mP·s) for the high-boiling PFPEs, which induced a high value of C_a ($C_a = \mu v / \gamma$) and a low value of viscosity ratios (λ where $\lambda = \mu_{disperse} / \mu_{continuous}$). This was undesirable for droplet formation because the interfacial velocity (γ / v) was not fast enough relative to v (m·s^{-1}) to relax the strained interface into forming droplets, in addition, it need large values of shear rate to rupture the interface at low viscosity ratios, which can generate high pressures with viscous PFPEs as carrier fluids [27,88,89].To solve this problem, Chan et al. designed a microdevice with a stepped microstructure increasing in channel height, as

shown in Figure 4. With this device, ODE droplets in Fomblin Y 06/6 PFPEs were generated at a flow-focusing orifice, and CdSe nanocrystals were produced when the droplets going through the glass microreactor had temperatures of 240–300 °C, although C_a was 0.81 and λ was 0.035.
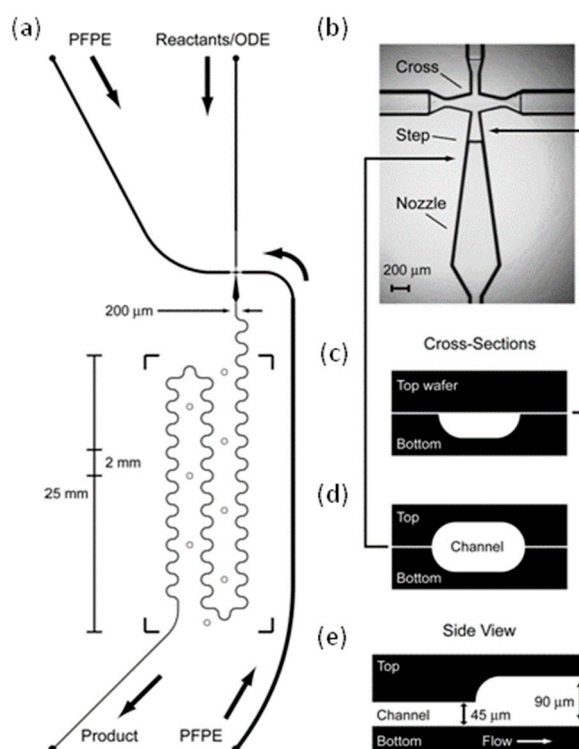
Figure 4. The microreactor channel design with droplet jet injector used by Chan et al. [87]: (**a**) Channel schematic showing dimensions, inlets (●), thermocouple wells (○), and boundaries of Kapton heater [87] (**b**) Optical micrograph of droplet injection cross. ODE is injected into the top channel, while the PFPE is injected in the side channels (**c**) Lateral "D"-shaped cross section of channel etched on the bottom wafer only (**d**) Cross-section of ellipsoidal channel etched on both top and bottom wafers. (**e**) Axial cross-section showing the 45 μm stepped up in channel height. Reproduced with permission from Chan, E.M., et al., *Journal of the American Chemical Society*; published by American Chemical Society, 2005.
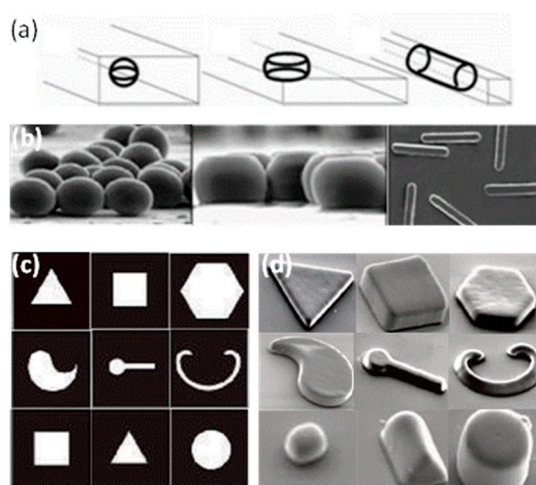
2.2. Non-Spherical Particles

Non-spherical particles offer unique properties compared to those of spherical particles [90–93]. For example, in optics, rod-shaped particles often have superior optical properties due to the optical antenna effect. Prior studies suggested that anisotropically shaped nanoparticles can avoid bio-elimination more effectively than spherical particles under the same conditions [94]. These findings are promising and will lead to additional studies on irregular shapes and corresponding applications [49,85,95–98]. Many strategies were developed to fabricate non-spherical particles, including template molding [99], seeded emulsion polymerization [100] and self-assembly [101]. However, these methods are still difficult for producing high quality, monodisperse, non-spherical particles with tailored geometries and shapes.

Recent advances in droplet microfluidic technologies offer new approaches for the fabrication of non-spherical particles. One approach is to confine the droplets in microfluidic channels with different sizes and shapes. If the volume of the droplet is larger than that of the largest sphere which could be accommodated in the channel, the droplet will be deformed into a disk, ellipsoid or a rod, and the non-spherical particles can be generated after they are solidified in the confined channel [49,102]. Another approach is through the combination of photo-chemistry and photomasking; the photomask

with desired patterns is used as a template for the final particles. When the droplet periodically flows through the mask, photo-initiated polymerization will occur. With this approach, polymer particles with complicated shapes can be generated [91,103].

Xu et al. produced particles with different sizes and shapes using the first method [49]. They produced monodisperse droplets in a flow-focusing device, shaped the droplets in the confined channel, and solidified these droplets in situ. This method is applicable to a variety of materials, such as gels, metals and polymers. Some products are shown in Figure 5a,b. Dendukuri et al. easily produced complex and multifunctional particles using the second approach [103]. They synthesized various shapes, such as polygonal shapes, non-symmetric or curved objects, and high-aspect-ratio objects, as shown in Figure 5c,d. The shape and the size of particle is only controlled by the mask, and the morphology and the chemistry of the particles can be independently chosen to form a large number of unique particles for applications in coding, drug delivery and biosensors.

Figure 5. Non-spherical particles formed using the two approaches. (**a**) The spherical droplets deformed by the confinement of the outlet channel; (**b**) The optical microscopy images of particles: ellipsoids, disks, rods with (**a**) approaches [49]. Reproduced with permission from Xu, S., et al., *Angewandte Chemie*; published by John Wiley and Sons, 2005; (**c**) The transparency mask used to make nonspherical particles; (**d**) The SEM images of corresponding particles with (**c**) approaches [103]. Reproduced with permission from Dendukuri, D., et al., *Nature Materials*; published by Nature Publishing Group, 2006.

## 3. Microparticles with Double or Multi-Emulsions as the Template

Double or multi-emulsions are droplets with smaller droplets encapsulated in larger drops. Core shell microparticles are typically made using double emulsion droplets as templates. Theoretically, micro-devices combined with co-flowing and/or flow-focusing geometries can easily produce monodisperse double or multiple droplets, most of which are capillary microfluidic devices, as shown in Figure 6. There are three fluids flowing in different capillaries, including the inner fluid in the injection capillary, the middle and the outer fluid in square capillary. The inner fluid is sheared by the middle fluid to form single droplets, and the middle fluid containing one or more single droplets is pinched off by the outer fluid to form double or multiple droplets. This technique eliminates the difficulties of precisely controlling the shell thickness, secondary nucleation and aggregation, and non-uniform in the traditional processes [104–106]. However, the precise size and morphology control in this technology is very important and still a challenge to the preparation of microparticles.
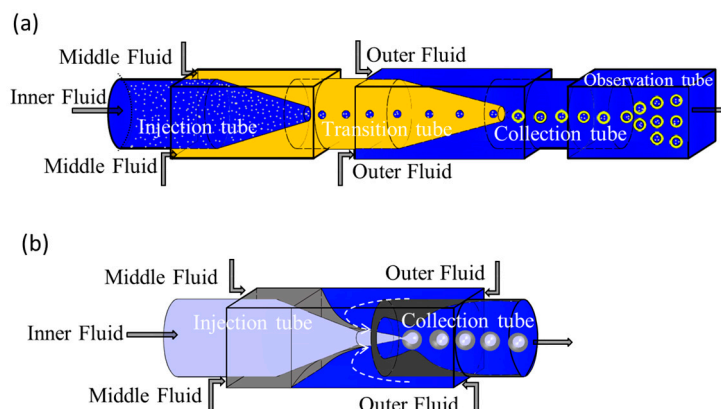
Figure 6. Fabricate of double emulsions in microfluidic devices. (**a**) Schematic of a capillary microfluidic device that combines double co-flowing geometry adapted from Figure 1 in [107]; (**b**) Schematic of a capillary microfluidic device that combines co-flow and flow-focusing geometry adapted from Figure 1 in [37].

3.1. Size Control of Core Shell Microparticles

Accurate control of the particle size is essential and in turn affects the release of inner active materials [108]. Dripping and jetting are two droplet formation regimes for each inner and middle fluid, as shown in Figure 7 [109]. The dripping regime may be the best choice to form a controllable core shell structure. The inner and outer drops should all be formed in the dripping regime to produce uniform microparticles, and the thickness of the shell can be precisely controlled.
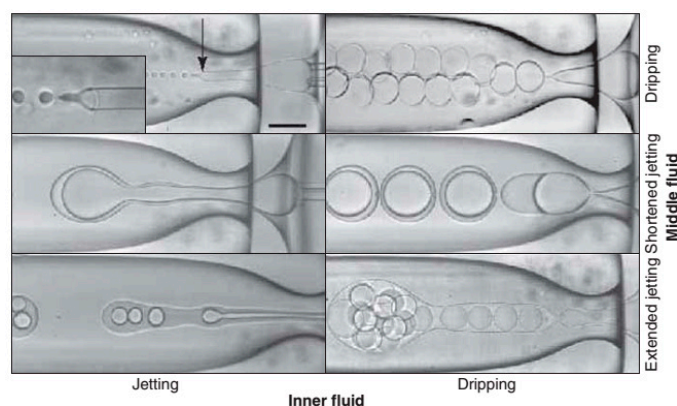

Figure 7. Different morphologies of double emulsions produced by a microcapillary device [109]. Reproduced with permission from Utada, A.S., et al., *MRS Bulletin*; published by Cambridge University Press, 2007.

Kim et al. used a microfluidic device to illustrate the predicted model of the radius droplet, as shown in Figure 8b [110]. At lower flow speeds, droplets will form in the dripping regime where droplets are very close to the orifice, and the mass flux is related to cross-sectional area. The size is controlled by the ratio of the flow rates of the sum of inner and middle fluids to the outer fluid (Q_{sum}/Q_{OF}). Equation (1) gives the relationship of the flow rate (Q) and each radius (R), where R_{thread} is the radius of the fluid thread that breaks into drops, and $R_{orifice}$ is the radius of the exit orifice. The values of $R_{thread}/R_{orifice}$ are predicted from Equation (1), with no adjustable parameters, and are consistent with the measured values in Figure 8a (open symbols). A comparison of the measured radii

of the drops and the thread shows that $R_{drop} = 1.82R_{thread}$ [111]. Based on the above research, R_{drop} can be predicted, which provides important guidance in creating double emulsions of a desired size.

$$\frac{Q_{sum}}{Q_{OF}} = \frac{\pi R_{thread}^2}{\pi R_{orifice}^2 - \pi R_{thread}^2} \tag{1}$$
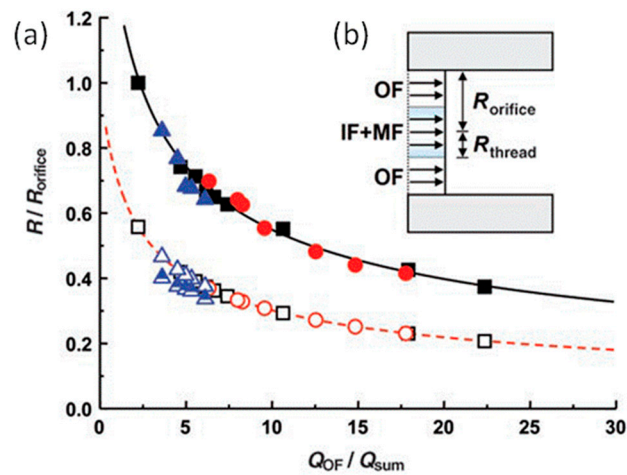
Figure 8. (**a**) Dependence of $R_{thread}/R_{orifice}$ on the scaled flow rate Q_{OF}/Q_{sum} [110]. The open symbols represent the R_{thread} for different liquids and double emulsions consisting of a single silicon drop surrounded by a liquid shell (3 $Q_{IF} = Q_{MF}$, triangle). The dashed line represents the predicted R_{thread}. R_{drop} values are represented with solid identical symbols. Half-filled triangles correspond to the radius of the internal droplets of the double emulsions. The solid line represents the predicted R_{drop}; (**b**) The flat velocity profile of the flow as it enters the capillary tube [110]. Reproduced with permission from Kim, J.W., et al., *Angewandte Chemie*; published by John Wiley and Sons, 2007.

Chang et al. designed a two co-axial capillaries microfluidic device to produce double droplets, from experiments they extracted an empirical law to predict core and shell sizes [112]. Since the core and the overall core shell drop has the same formation time, the core and the shell size could be predicted using the following equations, shown as Equations (2) and (3) (Q_I and Q_M are the inner and middle fluid flow rate respectively):

$$d_{core} = \sqrt[3]{\frac{Q_I}{Q_I + Q_M}} d_{drop} \tag{2}$$

$$d_{shell} = \frac{1}{2}(1 - \sqrt[3]{\frac{Q_I}{Q_I + Q_M}}) d_{drop} \tag{3}$$

3.2. Morphology Control of Core Shell Microparticles

As found by Dowding and Shum, when the polymer was formed by phase separation, the emulsion stabilizer had to be adjusted to control the particle morphology [113,114]. For combinations of a range of liquids, the final equilibrium morphology can be a core shell, or "acorn"-shaped, as shown in Figure 9. The transitions between different topologies of the double droplet can be described as the interfacial tensions model [115]. In the interfacial tension model, the balance of forces acting on the three-phase contact line is expressed in the form of relations (Neumann triangle Law, Figure 9a) between the contact angles and the interfacial tensions:

$$\gamma_{AB}\cos\theta_B + \gamma_B + \gamma_A(\theta_A + \theta_B) = 0 \tag{4}$$

$$\gamma_{AB}\cos\theta_A + \gamma_A + \gamma_B(\theta_A + \theta_B) = 0 \tag{5}$$
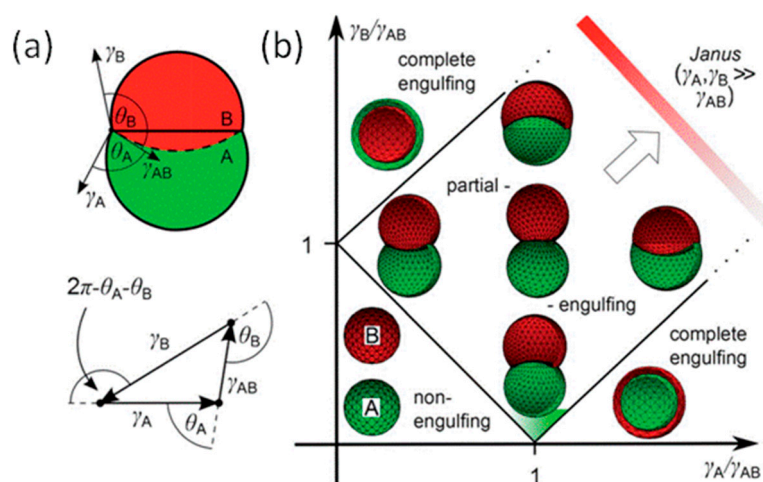
Figure 9. (**a**) Schematic of a double droplet with indicated contact angles θ_A and θ_B and the Neumann's triangle [115]; (**b**) Stability diagram representing the possible morphologies of a double droplet of phase A and B in the case $\kappa = V_B/V_A = 1$, κ is the ratio of the liquid volumes [115]. Reproduced with permission from Guzowski, J., et al., *Soft Matter*; published by Royal Society of Chemistry, 2012.

The existence and type of solution of Equations (4) and (5) depends on the values of the interfacial tensions. Guzowski and Korczyk used interfacial tensions to describe the transitions between different topologies of the droplets, marked by solid lines in Figure 9b [115]. They found three possible equilibrium topologies:

1. Complete-wetting: $\gamma_B > \gamma_{AB} + \gamma_A$, where a droplet of phase A is entirely encapsulated by phase B; vice versa ($\gamma_A > \gamma_{AB} + \gamma_B$), typical core shell structure;
2. Non-wetting: ($\gamma_{AB} > \gamma_A + \gamma_A$), droplets of phase A and B are separated by the outer phase;
3. Partial-wetting: droplets of phase A and B have a common interface and are both exposed to the external phase, corresponding to acorn-shaped or Janus.

This model has been generally applied to rationalize the particle morphologies observed when the polymer was caused to phase separate within the emulsified droplets, and in the presence of various core oils and aqueous emulsifier combinations [116]. By controlling the composition of the organic middle phase, the evolvement process will be conveniently transformed from initial core shell to the desired acorn-like configuration. Each of these morphologies has different potential applications. For example, the complete wetting state can be used for the encapsulation of active compounds, and partial wetting can be used to synthesize asymmetric and non-spherical functional particles [117].

3.3. Janus Particles

Janus particles are a class of anisotropic colloids, two sides of which have different compositions, polarities or surface modifications [117,118]. These particles have a wide range of potential applications in emulsion stabilization and dual-functionalized optical, electronic, sensor devices and incompatible drug delivery [119–123]. The "Janus" term has been also used for describing asymmetric dendritic macromolecules or unimolecular micelles based on block copolymers in solutions. Nevertheless, we will focus on hard and permanent Janus structures in this review, including biocompartmental, dumbbell-like, snowman-like, acorn-like and half-raspberry-like particles, as shown as Figure 10. In terms of materials, the reported Janus includes hydrogels and amphiphilic Janus.
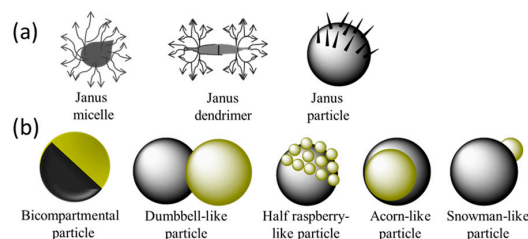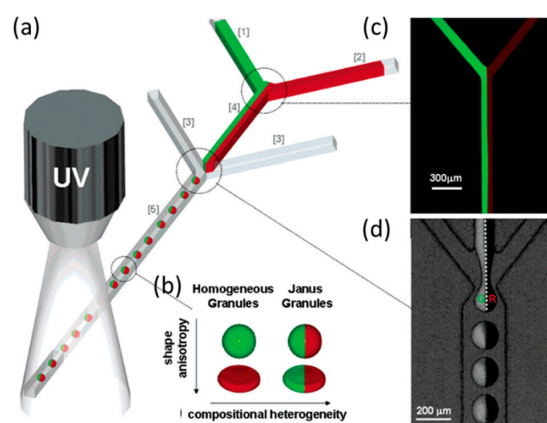
Figure 10. Schematic representation of Janus-like morphologies. (**a**) Extended Janus morphologies; (**b**) Solid Janus particles. (Note: spheres symbolize particles, diamonds and triangles symbolize chemical functions).

3.3.1. Hydrogel Janus

Hydrogel Janus is composed of two hydrogel phases produced from two completely immiscible hydrophilic monomer fluids. Unlike the principle for fabricating homogeneous particles, here, two separate streams are co-flowing through the same channel of the microfluidic device. However, the two fluids must remain parallel and the interface between them must be stable at different temporal and spatial scales, and any perturbations can lead to the formation of particles with mixed internal morphologies instead of particles with two distinct sides [24].

Shepherd and Conrad reported a scalable microfluidic assembly route for creating monodisperse silica colloid-filled hydrogel Janus [124]. Drops were formed by shearing a concentrated silica colloid-acrylamide aqueous suspension in a continuous oil phase using a sheath-flow device, as shown in Figure 11. Then, they immobilized the colloids within each drop by photo polymerizing the acrylamide to form a hydrogel. Seiffert et al. demonstrated a microfluidic technique to produce functional Janus microgels from prefabricated, cross-linkable precursor polymers [125]. This approach separated the particle formation from the synthesis of the polymer material, which allowed the droplet templating and functionalization of the matrix polymer to be controlled independently. Therefore, Janus particles were created with very specific, well-defined modifications of the two sides, even on a molecular level. In addition, they fabricated hollow microcapsules with two different sides (Janus shells), using the method as shown in Figure 12, and the size of the resultant droplets were controlled by adjusting the fluid flow rates and channel geometry.

Figure 11. (**a**) Schematic representation of sheath-flow microfluidic device used to produce monodisperse colloid-filled hydrogel granules; (**b**) Schematic view of granule shapes and compositions explored; (**c**) Fluorescent image of Y-junction formed by inlets [1,2] for the production of Janus spheres; (**d**) Backlit fluorescence image (green excitation) illustration that the fluorescein isothiocyanate (FITC)-silica microspheres remain sequestered in the left hemisphere of each granule generated. Pictures are from [124]. Reproduced with permission from Shepherd, R.F., et al., *Langmuir*; published by American Chemical Society, 2006.
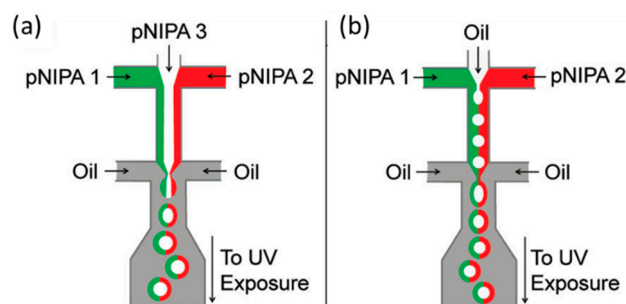
Figure 12. Formation of Janus microgels and microshells [125]. (**a**) Schematic of a microfluidic device forming aqueous droplets from three independent semidilute pNIPPAm solutions. The center phase (white) is assembled in the core of the droplets, whereas the right- and left-flowing phases (red and green) form the shell (**b**) operating the device in a modified way yields oil-water-oil double emulsions with Janus-shaped middle phases. Reproduced with permission from Seiffert, S., et al., *Langmuir*; published by American Chemical Society, 2010.

Although the mixing between liquids in a laminar flow was weak, it was enhanced by the hydrodynamic focusing of liquid threads before the break-up into droplets, which led to a gradual change in composition along the direction normal to the interface [126]. This limits the Janus application since a sharp interface between the phases is required.

3.3.2. Amphiphilic Janus

Amphiphilic Janus is formed from different immiscible fluids using double-emulsion droplets as templates. This method eliminates the problem of the mixing in the interface, however, the interfacial tension γ or spreading coefficients S_i must be within a certain range to assure the stability of double droplets within the partial-wetting area (in Figure 9). Thus, the portfolio of chemicals from a broad range of immiscible fluids is a key problem in the preparation of Janus particles.

Chen et al. fabricated acorn-like particles using W/O/W double emulsions as templates in PDMS microfluidic devices [80]. Moreover, the inner and the outer droplet size were adjusted by varying each fluid flow rate, and the swelling of the particles was controlled by varying the cross-linker concentration. Dendukuri et al. reported the synthesis and self-assembly of wedge-shaped particles bearing segregated hydrophilic and hydrophobic sections using continuous flow lithography technology (CFL) [127]. Monodisperse dumbbell-like hybrid Janus microspheres with organic and inorganic parts were prepared using fused perfluoroplyethers (the organic phase) and hydrolytic allylhydridopolycarbosilane (the inorganic phase) droplets as the template in a cross-flowing microfluidic device [128]. The particles had distinctive surface properties. The hydrophobic hemisphere had a smooth surface and the hydrophilic region had a rough, porous surface.

3.4. Microcapsules

Microcapsules are commonly used in pharmaceuticals, foods, cosmetics and absorbent [85,129–131]. The solid polymer shells provide effective encapsulation, protect the encapsulated drug or the active materials from hazardous environmental conditions, and give a release profile for a desired period. Though solid microspheres can also be used as drug delivery supporters, the drug distribution is largely dependent on the microsphere size [132,133], and the active-release mechanism is the diffusion-degradation [57], which limits improvement for medication compliance.

Microcapsules provide another way to control the drug-release rate and the release mechanism [2,90]. First, when a drug is localized in the core matrices, the shell prolongs the diffusion path of water-in and drug-out, and hence lowers the initial burst release [134]. Second, altering the properties of the shell, such as the shell thickness, may change the active transport kinetics [90]. For example, when increasing the polylactic acid (PLA) shell thickness to 10μm, the release profile

will shift from a biphasic shape for pure PLGA microspheres to a zero-order piroxicam release [135]. However, it is still difficult to produce a microcapsule with a predicted size and morphology.

Equations (1)–(3) show a quantitative analysis of the relationship between the flow rate and the diameters of the inner and outer drops, and predicts the number of inner droplets [62,112]. Chu and Utada fabricated highly monodisperse multiple emulsions with controlled sizes and inner structures using capillary microfluidics, and obtained a liner relationship between the relative flow rate with drop diameters for both the inner and outer drops, and with the number of encapsulated droplets in the double emulsions [136]. By simply incorporating alternate emulsification schemes, more complicated multiple emulsions and microcapsules can be fabricated, as shown in Figure 13.
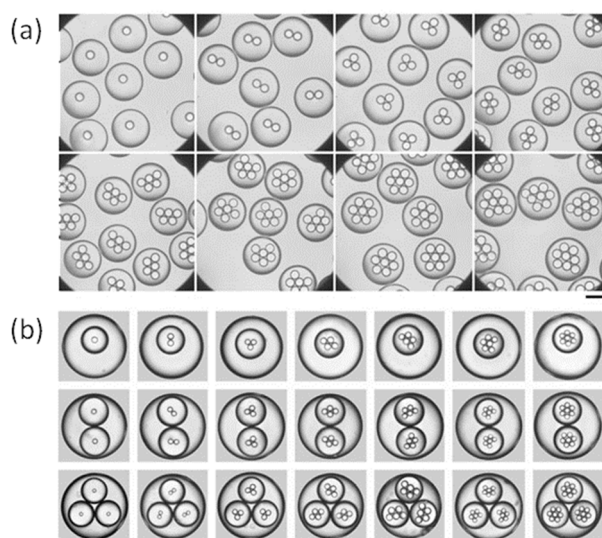
Figure 13. (**a**) Optical micrographs of double emulsions that contain a controlled number of inner droplets; (**b**) Optical micrographs of triple emulsions that contain a controlled number of inner and middle droplets. The scale bar in all images is 200 μm. Pictures are from [136]. Reproduced with permission from Chu, L.-Y., et al., *Angewandte Chemie International Edition*; published by John Wiley and Sons, 2007.

Carbon microspheres are of great interest due to their potential applications as cellular delivery vehicles, drug delivery carriers and absorbents [137–140]. Zhang et al. prepared monodisperse poly(furfuryl alcohol) (PFA) hollow microspheres by the microfluidic technique in a T-junction device through interfacial polymerization of FA in H_2SO_4 solution droplets. After pyrolysis, they produced carbon microspheres with mean particle sizes of 0.7–1.2 μm [141,142]. If some solid nanobeads or microbeads are added in the inner fluid, this method can be adapted to make microcapsules with controlled holes [107]. Other functional nanoparticles such as SiO_2, Au, Co, Fe_3O_4 and fluorescence nanoparticles have been introduced into the inner fluid to fabricate functional microcapsules [117,143,144].

3.5. Vesicles

An ideal encapsulating structure should not only have high encapsulation efficiency, but also should be easily triggered to release the actives. Vesicles are a good choice for an encapsulating structure. Vesicles are a compartment of one fluid enclosed by a bilayer of amphiphilic molecules, such as phospholipids, polypeptides and diblock copolymers, which correspond to liposomes and polymersomes. The bilayer membrane can encapsulate hydrophilic and hydrophobic molecules simultaneously. Thus multiple drugs with different properties stored in a single carrier can be released at the same time. The bilayer membrane also induces semi-permeability of small molecules, such as

water, leading to inflated or deflated responses to osmotic pressure differences between the aqueous core and surrounding environment.

Liposomes are biocompatible vesicles with phospholipid bilayers. They have attracted much attention because phospholipids constitute the majority of biological membranes found in nature, such as plasma membranes. Thus, they have great potential for encapsulation and targeted drug delivery considering their biocompatible properties. The disadvantage is that they are more fragile than polymersomes, and their preparation is more delicate.

Lorenceau and Utada [37] used water in oil in water (W/O/W) double emulsions as templates to form monodisperse polymersomes by using a diblock copolymer poly(normal-butyl acrylate)-poly(acrylic acid) (PBA-PAA) in a capillary microfluidic device. The amphiphilic PBA-PAA in the middle fluid stabilized the two oil-water interfaces, and self-assembled on the interface during the dewetting oil phase upon solvent evaporation. The concentration of the amphiphilic molecules was a key control variable in the fabrication of polymersomes in this fabrication process [38]. If the concentration was lower than the amount required to fully cover the interfaces, the polymersomes were unstable. However, too much excess created a depletion interaction.

By integrating the advantages of the diblock copolymer and the microdroplet based-on microfluidic technology, the polymersome can be easily fabricated with excellent encapsulation efficiency, high levels of loading and tunable wall properties. For example, since the three fluids can be controlled individually, the encapsulate can contain the same amount of active material in each polymersomes and guarantee that the encapsulation efficiency will reach 100% [38]. In addition, the character of each block in the diblock copolymer can be tuned to fit the desired application. For example, tuning the molecular weight ratio of the hydrophilic and the hydrophobic blocks, the wetting angle of the polymer-containing solvent phase on the polyersomes will change in the emulsion-to-vesicles transition [114], as shown in Figure 14. The polymerization degree of the individual diblock molecules will affect the membrane thickness, whereas the elasticity and permeability of the membrane can be adjusted by changing the glass transition temperature of the hydrophobic block [145–147].
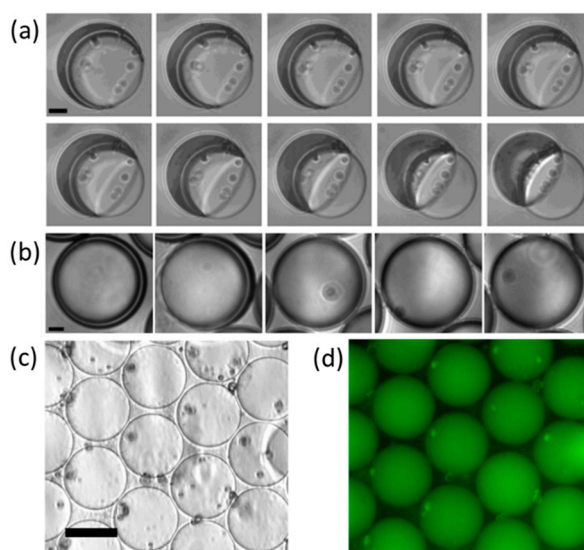
Figure 14. (**a**) Bright-field microscope images of a PEG(5000)-b-PLA(5000) polymersome undergoing dewetting transition; (**b**) Bright-field microscope images of a PEG(1000)-b-PLA(5000) polymersome undergoing the evaporation of the organic solvent shell; (**c**,**d**) Bright-field and fluorescence microscope images of a dried capsule formed from the PEG(1000)-b-PLA(5000) diblock copolymer. Pictures are from [114]. Reproduced with permission from Shum, H.C., et al., *Journal of the American Chemical Society*; published by American Chemical Society, 2008.

Core shell structured fibers are also excellent delivery vehicles for medicines. Wang et al. fabricated fibers with core shell structures by emulsion electrospinning [148]. The water in oil (W/O) emulsions were composed of deionized water or a phosphate buffer saline, and a poly(lactic-co-glycolic acid) (PLGA)/chloroform solution that contained a surfactant was used as a module to produce core shell structured fibers. This study demonstrated the evolution of the core shell structured fibers by investigating the water phase morphology in jets or fibers at different locations of the jet or fiber trajectory during the electrospinning process, as shown in Figure 15. They found that the water phase in emulsion jets experienced multi-level stretching and broke up. The Rayleigh capillary instability and the solvent evaporation rate significantly affected the breakup of water droplets.
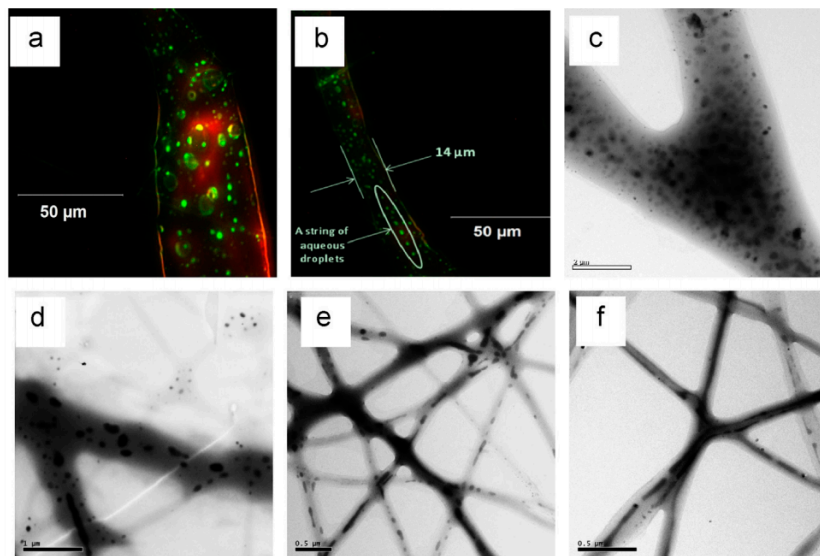
Figure 15. Morphological evaluation of the water phase in electrospun fibers collected at different locations of the emulsion jet path: (**a**,**b**) fluorescence microscopy images of fibers; (**c**–**f**) TEM micrographs at different magnifications. Pictures are from [148]. Reproduced with permission from Wang, C., et al., *Materials Letters*; published by Elsevier, 2014.

Since the mechanical properties of core shell microparticles made from materials with dramatically different elastic properties are also important factors in medical applications, the mechanical properties of these microparticles were measured and predicted by a microfluidic approach [149]. By forcing the particles through a tapered capillary and analyzing their deformation, the shear and compressive moduli were easily measured in one single experiment. The results showed that the moduli of these core shell structures were determined both by the material composition of the core shell microparticles and by their microstructures.

4. Conclusions

Droplet microfluidics can provide environments with properties of exceptional control and good stability, which can be used for performing microparticles synthesis with unique properties. We reviewed the different microfluidic systems for controlling droplet formation, the influencing factors for regulating droplet size and structure, and droplets solidification methods according to different materials. To make the applications of droplet microfluidics in preparation of micro- and nanoparticles more clear, we introduced the preparation methods of different materials, different structures and different functional microspheres in detail. Because these particles are characterized by particle size uniformity, structure controllability and component controllability, they are more widely applicable than those prepared by traditional methods, especially in new medicine (embolization treatment of tumor, drug controlled-release, multi-drug loading microspheres), adsorption separation,

dual-functionalized optical, electrical and magnetic devices, etc. This technique has become a powerful platform in material fabrication, and biological and medical research. However, one obstacle in the practical application in microparticles preparation is their low-throughput, which limits the production efficiency. Recent advances have partially overcome this barrier by parallelizing droplet generation and enhanced the production rate by a factor of 100, but these parallel experiments were used primarily for the generation of spherical single droplets and didnot report on the generation of non-spherical, double or multi-emulsion, and nor did perform on droplets in situ curing parallelization. More efforts are needed to resolve these technical issues. Given the distinctive properties of this technique and its tremendous demand in applications, droplet microfluidics will fundamentally modify the future of micro- and nano-manufacturing and drug delivery.

Author Contributions: Jianmei Wang was mainly involved in writing the manuscript; Chengyang Wang and Liqiu Wang conceived and reviewed the manuscipt; Yan Li contributed in discussion and helped modify the manuscript; Xueying Wang and Jianchun Wang helped drawing the figures; Hanmei Tian, Pei Zhao, Ye Tian and Yeming Gu helped searching the literatures.

Conflicts of Interest: The authors declare no conflict of interest.

References

1.　Cazado, C.P.S.; Pinho, S.C.D. Effect of different stress conditions on the stability of quercetin-loaded lipid microparticles produced with babacu (*Orbignya speciosa*) oil: Evaluation of their potential use in food applications. *Food Sci. Technol.* **2016**. ahead. [CrossRef]

2.　Wu, J.; Kong, T.; Yeung, K.W.K.; Shum, H.C.; Cheung, K.M.C.; Wang, L.; To, M.K.T. Fabrication and characterization of monodisperse PLGA–alginate core–shell microspheres with monodisperse size and homogeneous shells for controlled drug release. *Acta Biomater.* **2013**, *9*, 7410–7419. [CrossRef] [PubMed]

3.　Nidhi, R.M.; Kaur, V.; Hallan, S.S.; Sharma, S.; Mishra, N. Microparticles as controlled drug delivery carrier for the treatment of ulcerative colitis: A brief review. *Saudi Pharm. J.* **2016**, *24*, 458–472. [CrossRef] [PubMed]

4.　Elsherbiny, I.M.; Abbas, Y. Janus Nano- and Microparticles as Smart Drug Delivery Systems. *Curr. Pharm. Biotechnol.* **2016**, *17*, 673–682. [CrossRef]

5.　Shen, Y.; Zhao, Q.; Li, X.; Zhang, D. Monodisperse $Ca_{0.15}Fe_{2.85}O_4$ microspheres: Facile preparation, characterization, and optical properties. *J. Mater. Sci.* **2012**, *47*, 3320–3326. [CrossRef]

6.　Yamada, H.; Nakamura, T.; Yamada, Y.; Yano, K. Colloidal-Crystal Laser Using Monodispersed Mesoporous Silica Spheres. *Adv. Mater.* **2009**, *21*, 4134–4138. [CrossRef]

7.　Horák, D.; Kučerová, J.; Korecká, L.; Jankovi, B.; Mikulášek, P.; Bílková, Z. New Monodisperse Magnetic Polymer Microspheres Biofunctionalized for Enzyme Catalysis and Bioaffinity Separations. *Macromol. Biosci.* **2012**, *12*, 647–655. [CrossRef] [PubMed]

8.　Fang, Q.; Cheng, Q.; Xu, H.; Xuan, S. Monodisperse magnetic core/shell microspheres with Pd nanoparticles-incorporated-carbon shells. *Dalton Trans.* **2013**, *43*, 2588–2595. [CrossRef] [PubMed]

9.　Deng, Y.; Cai, Y.; Sun, Z.; Liu, J.; Liu, C.; Wei, J.; Li, W.; Liu, C.; Wang, Y.; Zhao, D. Multifunctional mesoporous composite microspheres with well-designed nanostructure: A highly integrated catalyst system. *J. Am. Chem. Soc.* **2010**, *132*, 8466–8473. [CrossRef] [PubMed]

10.　Sang, E.S.; Yang, S.; Choi, H.H.; Choe, S. Fully crosslinked poly(styrene-co-divinylbenzene) microspheres by precipitation polymerization and their superior thermal properties. *J. Polym. Sci. Part A Polym. Chem.* **2004**, *42*, 835–845.

11.　Goh, E.C.C.; Stöver, H.D.H. Cross-Linked Poly(methacrylic acid-co-poly(ethylene oxide) methyl ether methacrylate) Microspheres and Microgels Prepared by Precipitation Polymerization: A Morphology Study. *Macromolecules* **2002**, *35*, 9983–9989. [CrossRef]

12. Chu, Y.; Zhang, P.; Hu, J.; Yang, W.; Wang, C. Synthesis of Monodispersed Co(Fe)/Carbon Nanocomposite Microspheres with Very High Saturation Magnetization. *J. Phys. Chem C* **2009**, *113*, 4047–4052. [CrossRef]

13. Li, Y.; Chen, J.; Xu, Q.; He, L.; Chen, Z. Controllable Route to Solid and Hollow Monodisperse Carbon Nanospheres. *J. Phys. Chem. C* **2009**, *113*, 10085–10089. [CrossRef]

14. Choi, J.; Kwak, S.Y.; Kang, S.; Lee, S.S.; Park, M.; Lim, S.; Kim, J.; Choe, C.R.; Hong, S.I. Synthesis of highly crosslinked monodisperse polymer particles: Effect of reaction parameters on the size and size distribution. *J. Polym. Sci. Part A Polym. Chem.* **2002**, *40*, 4368–4377. [CrossRef]

15. Lee, J.; Ha, J.U.; Choe, S.; Lee, C.S.; Shim, S.E. Synthesis of highly monodisperse polystyrene microspheres via dispersion polymerization using an amphoteric initiator. *J. Colloid Interface Sci.* **2006**, *298*, 663–671. [CrossRef] [PubMed]

16. Akamatsu, K.; Chen, W.; Suzuki, Y.; Ito, T.; Nakao, A.; Sugawara, T.; Kikuchi, R.; Nakao, S. Preparation of monodisperse chitosan microcapsules with hollow structures using the SPG membrane emulsification technique. *Langmuir ACS J. Surf. Colloids* **2010**, *26*, 14854–14860. [CrossRef] [PubMed]

17. Feng, Q.; Wu, J.; Yang, T.; Ma, G.; Su, Z. Mechanistic studies for monodisperse exenatide-loaded PLGA microspheres prepared by different methods based on SPG membrane emulsification. *Acta Biomater.* **2014**, *10*, 4247–4256.

18. Caruso, F.; Spasova, M.; Susha, A.; Giersig, M.; Caruso, R.A. Magnetic Nanocomposite Particles and Hollow Spheres Constructed by a Sequential Layering Approach. *Chem. Mater.* **2001**, *13*, 109–116. [CrossRef]

19. Tan, S.H.; Maes, F.; Semin, B.; Vrignon, J.; Baret, J.C. The Microfluidic Jukebox. *Sci. Rep.* **2014**, *4*, 597–600. [CrossRef] [PubMed]

20. Tan, S.H.; Nguyen, N.T. Generation and manipulation of monodispersed ferrofluid emulsions: The effect of a uniform magnetic field in flow-focusing and T-junction configurations. *Phys. Rev. E* **2011**, *84*, 2299–2304. [CrossRef] [PubMed]

21. Zeng, S.; Li, B.; Su, X.; Qin, J.; Lin, B. Microvalve-actuated precise control of individual droplets in microfluidic devices. *Lab Chip* **2009**, *9*, 1340–1343. [CrossRef] [PubMed]

22. Ma, Z.; Teo, A.; Tan, S.; Ai, Y.; Nguyen, N.T. Self-Aligned Interdigitated Transducers for Acoustofluidics. *Micromachines* **2016**, *7*, 216. [CrossRef]

23. Tan, S.-H.; Sohel Murched, S.M.; Nguyen, N.-T.; Neng, T.N.; Wong, T.; Yobas, L. Thermally controlled droplet formation in flow focusing geometry: Formation regimes and effect of nanoparticle suspension. *J. Phys. D Appl. Phys.* **2008**, *41*, 165501. [CrossRef]

24. Nisisako, T.; Torii, T.; Takahashi, T.; Takizawa, Y. Synthesis of Monodisperse Bicolored Janus Particles with Electrical Anisotropy Using a Microfluidic Co-Flow System. *Adv. Mater.* **2006**, *18*, 1152–1156. [CrossRef]

25. Othman, R.; Vladisavljević, G.T.; Bandulasena, H.C.H.; Nagy, Z.K. Production of polymeric nanoparticles by micromixing in a co-flow microfluidic glass capillary device. *Chem. Eng. J.* **2015**, *280*, 316–329. [CrossRef]

26. Dang, T.D.; Kim, Y.H.; Kim, H.G.; Kim, G.M. Preparation of monodisperse PEG hydrogel microparticles using a microfluidic flow-focusing device. *J. Ind. Eng. Chem.* **2012**, *18*, 1308–1313. [CrossRef]

27. Anna, S.L.; Bontoux, N.; Stone, H.A. Formation of dispersions using "flow focusing" in microchannels. *Appl. Phys. Lett.* **2003**, *82*, 364–366. [CrossRef]

28. Cohen, C.; Giles, R.; Sergeyeva, V.; Mittal, N.; Tabeling, P.; Zerrouki, D.; Baudry, J.; Bibette, J.; Bremond, N. Parallelised production of fine and calibrated emulsions by coupling flow-focusing technique and partial wetting phenomenon. *Microfluid. Nanofluid.* **2016**, *17*, 959–966. [CrossRef]

29. Garstecki, P.; Fuerstman, M.J.; Stone, H.A.; Whitesides, G.M. Formation of droplets and bubbles in a microfluidic T-junction-scaling and mechanism of break-up. *Lab Chip* **2006**, *6*, 437–446. [CrossRef] [PubMed]

30. Wu, Y.; Fu, T.; Ma, Y.; Li, H.Z. Active control of ferrofluid droplet breakup dynamics in a microfluidic T-junction. *Microfluid. Nanofluid.* **2015**, *18*, 19–27. [CrossRef]

31. Chokkalingam, V.; Herminghaus, S.; Seemann, R. Self-synchronizing pairwise production of monodisperse droplets by microfluidic step emulsification. *Appl. Phys. Lett.* **2008**, *93*. [CrossRef]

32. Kobayashi, I.; Nakajima, M.; Nabetani, H.; Kikuchi, Y.; Shohno, A.; Satoh, K. Preparation of micron-scale monodisperse oil-in-water microspheres by microchannel emulsification. *J. Am. Oil Chem. Soc.* **2001**, *78*, 797–802. [CrossRef]

33. Khalid, N.; Kobayashi, I.; Neves, M.A.; Uemura, K.; Nakajima, M.; Nabetani, H. Monodisperse W/O/W emulsions encapsulating L-ascorbic acid: Insights on their formulation using microchannel emulsification and stability studies. *Colloids Surf. A Physicochem. Eng. Asp.* **2014**, *458*, 69–77. [CrossRef]

34. Kang, D.-K.; Monsur Ali, M.; Zhang, K.; Pone, E.J.; Zhao, W. Droplet microfluidics for single-molecule and single-cell analysis for cancer research, diagnosis and therapy. *TrAC Trends Anal. Chem.* **2014**, *58*, 145–153. [CrossRef]

35. Streets, A.M.; Huang, Y. Microfluidics for biological measurements with single-molecule resolution. *Curr. Opin. Biotechnol.* **2014**, *25*, 69–77. [CrossRef] [PubMed]

36. Thorsen, T.; Roberts, R.W.; Arnold, F.H.; Quake, S.R. Dynamic Pattern Formation in a Vesicle-Generating Microfluidic Device. *Phys. Rev. Lett.* **2001**, *86*, 4163–4166. [CrossRef] [PubMed]

37. Utada, A.; Lorenceau, E.; Link, D.; Kaplan, P.; Stone, H.; Weitz, D. Monodisperse double emulsions generated from a microcapillary device. *Science* **2005**, *308*, 537–541. [CrossRef] [PubMed]

38. Shah, R.K.; Shum, H.C.; Rowat, A.C.; Lee, D.; Agresti, J.J.; Utada, A.S.; Chu, L.-Y.; Kim, J.-W.; Fernandez-Nieves, A.; Martinez, C.J.; Weitz, D.A. Designer emulsions using microfluidics. *Mater. Today* **2008**, *11*, 18–27. [CrossRef]

39. Zhang, H.; Tumarkin, E.; Sullan, R.M.A.; Walker, G.C.; Kumacheva, E. Exploring Microfluidic Routes to Microgels of Biological Polymers. *Macromol. Rapid Commun.* **2007**, *28*, 527–538. [CrossRef]

40. Zhao, C.X.; Middelberg, A.P.J. Two-phase microfluidic flows. *Chem. Eng. Sci.* **2011**, *66*, 1394–1411. [CrossRef]

41. Chong, Z.Z.; Tan, S.H.; Gañán-Calvo, A.M.; Tor, S.B.; Loh, N.H.; Nguyen, N.T. Active droplet generation in microfluidics. *Lab Chip* **2016**, *16*, 35. [CrossRef] [PubMed]

42. Zhu, P.; Wang, L. Passive and active droplet generation with microfluidics: A review. *Lab Chip* **2017**, *17*, 34–75. [CrossRef] [PubMed]

43. Zeng, Y.; Shin, M.; Wang, T. Programmable active droplet generation enabled by integrated pneumatic micropumps. *Lab Chip* **2012**, *13*, 267–273. [CrossRef] [PubMed]

44. Beer, N.R.; Wheeler, E.K.; Leehoughton, L.; Watkins, N.; Nasarabadi, S.; Hebert, N.; Leung, P.; Arnold, D.W.; Bailey, C.G.; Colston, B.W. On-chip single-copy real-time reverse-transcription PCR in isolated picoliter droplets. *Anal. Chem.* **2007**, *80*, 1854–1858. [CrossRef] [PubMed]

45. Willingale, J.; Manzarpour, A.; Mantle, P.G. Continuous synthesis of gold nanoparticles in a microreactor. *Nano Lett.* **2005**, *5*, 685–691.

46. Chu, L.Y.; Kim, J.W.; Shah, R.K.; Weitz, D.A. Monodisperse Thermoresponsive Microgels with Tunable Volume-Phase Transition Kinetics. *Adv. Funct. Mater.* **2007**, *17*, 3499–3504. [CrossRef]

47. Lee, I.; Yoo, Y.; Cheng, Z.; Jeong, H.K. Generation of monodisperse mesoporous silica microspheres with controllable size and surface morphology in a microfluidic device. *Adv. Funct. Mater.* **2008**, *18*, 4014–4021. [CrossRef]

48. Datta, S.S.; Abbaspourrad, A.; Amstad, E.; Fan, J.; Kim, S.H.; Romanowsky, M.; Shum, H.C.; Sun, B.; Utada, A.S.; Windbergs, M. 25th anniversary article: Double emulsion templated solid microcapsules: Mechanics and controlled release. *Adv. Mater.* **2014**, *26*, 2205–2218. [CrossRef] [PubMed]

49. Xu, S.; Nie, Z.; Seo, M.; Lewis, P.; Kumacheva, E.; Stone, H.A.; Garstecki, P.; Weibel, D.B.; Gitlin, I.; Whitesides, G.M. Generation of monodisperse particles by using microfluidics: Control over size, shape, and composition. *Angew. Chem.* **2005**, *117*, 734–738. [CrossRef]

50. Pelage, J.-P.; Laurent, A.; Wassef, M.; Bonneau, M.; Germain, D.; Rymer, R.; Flaud, P.; Martal, J.; Merland, J.J. Uterine Artery Embolization in Sheep: Comparison of Acute Effects with Polyvinyl Alcohol Particles and Calibrated Microspheres. *Radiology* **2002**, *224*, 436–445. [CrossRef] [PubMed]

51. Gomes, A.S.; Rosove, M.H.; Rosen, P.J.; Amado, R.G.; Sayre, J.W.; Monteleone, P.A.; Busuttil, RW. Triple-drug transcatheter arterial chemoembolization in unresectable hepatocellular carcinoma: Assessment of survival in 124 consecutive patients. *Am. J. Roentgenol.* **2009**, *193*, 1665–1671. [CrossRef] [PubMed]

52. Beaujeux, R.; Laurent, A.; Wassef, M.; Casasco, A.; Gobin, Y.-P.; Aymard, A.; Rüfenacht, D.; Merland, J.J. Trisacryl gelatin microspheres for therapeutic embolization, II: Preliminary clinical evaluation in tumors and arteriovenous malformations. *Am. J. Neuroradiol.* **1996**, *17*, 541–548. [PubMed]

53. Carugo, D.; Capretto, L.; Willis, S.; Lewis, A.L.; Grey, D.; Hill, M.; Zhang, X. A microfluidic device for the characterisation of embolisation with polyvinyl alcohol beads through biomimetic bifurcations. *Biomed. Microdevice* **2012**, *14*, 153–163. [CrossRef] [PubMed]

54. Kong, T.; Wu, J.; To, M.; Wai Kwok Yeung, K.; Cheung Shum, H.; Wang, L. Droplet based microfluidic fabrication of designer microparticles for encapsulation applications. *Biomicrofluidics* **2012**, *6*, 34104. [CrossRef] [PubMed]

55. Lai, B.; Wei, Q.; Sun, C.-B.; Ma, G.-H.; Su, Z.-G. Preparation of Uniform-sized PELA Microspheres Containing Lysozyme by Membrane Emulsification and Double Emulsion-Solvent Removal Method. *Chin. J. Process Eng.* **2008**, *8*, 327–332.

56. Vladisavljević, G.T.; Schubert, H. Influence of process parameters on droplet size distribution in SPG membrane emulsification and stability of prepared emulsion droplets. *J. Membr. Sci.* **2003**, *225*, 15–23. [CrossRef]

57. Berkland, C.; Kipper, M.J.; Narasimhan, B.; Kim, K.K.; Pack, D.W. Microsphere size, precipitation kinetics and drug distribution control drug release from biodegradable polyanhydride microspheres. *J. Control. Release* **2004**, *94*, 129–141. [CrossRef] [PubMed]

58. Xu, Q.; Hashimoto, M.; Dang, T.T.; Hoare, T.; Kohane, D.S.; Whitesides, G.M.; Langer, R.; Anderson, D.G. Preparation of Monodisperse Biodegradable Polymer Microparticles Using a Microfluidic Flow-Focusing Device for Controlled Drug Delivery. *Small* **2009**, *5*, 1575–1581. [CrossRef] [PubMed]

59. Seo, M.; Nie, Z.; Xu, S.; Mok, M.; Lewis, P.C.; Graham, R.; Kumacheva, E. Continuous Microfluidic Reactors for Polymer Particles. *Langmuir* **2005**, *21*, 11614–11622. [CrossRef] [PubMed]

60. Serra, C.; Berton, N.; Bouquey, M.; Prat, L.; Hadziioannou, G. A Predictive Approach of the Influence of the Operating Parameters on the Size of Polymer Particles Synthesized in a Simplified Microfluidic System. *Langmuir* **2007**, *23*, 7745–7750. [CrossRef] [PubMed]

61. Theberge, A.B.; Courtois, F.; Schaerli, Y.; Fischlechner, M.; Abell, C.; Hollfelder, F.; Huck, W.S.T. Microdroplets in Microfluidics: An Evolving Platform for Discoveries in Chemistry and Biology. *Angew. Chem. Int. Ed.* **2010**, *49*, 5846–5868. [CrossRef] [PubMed]

62. Abate, A.R.; Seiffert, S.; Utada, A.S.; Shum, A.; Shah, R.; Thiele, J.; Duncanson, W.J.; Abbaspourad, A.; Lee, M.H.; Akartuna, I.; et al. Microfluidic Techniques for Synthesizing Particles. Available online: http://weitzlab.seas.harvard.edu/publications/Bookchapter_Microfluidic_techniques.pdf (accessed on 13 January 2017).

63. Pankhurst, Q.A.; Connolly, J.; Jones, S.K.; Dobson, J. Applications of magnetic nanoparticles in biomedicine. *J. Phys. D Appl. Phys.* **2003**, *36*, R167. [CrossRef]

64. Fleischmann, E.K.; Ohm, C.; Serra, C.; Zentel, R. Preparation of Soft Microactuators in a Continuous Flow Synthesis Using a Liquid-Crystalline Polymer Crosslinker. *Macromol. Chem. Phys.* **2012**, *213*, 1871–1878. [CrossRef]

65. Ohm, C.; Fleischmann, E.K.; Kraus, I.; Serra, C.; Zentel, R. Control of the Properties of Micrometer-Sized Actuators from Liquid Crystalline Elastomers Prepared in a Microfluidic Setup. *Adv. Funct. Mater.* **2010**, *20*, 4314–4322. [CrossRef]

66. Muvaffak, A.; Gurhan, I.; Gunduz, U.; Hasirci, N. Preparation and characterization of a biodegradable drug targeting system for anticancer drug delivery: Microsphere-antibody conjugate. *J. Drug Target.* **2005**, *13*, 151–159. [CrossRef] [PubMed]

67. Amesur, N.; Zajko, A.; Carr, B. Chemo-embolization for Unresectable Hepatocellular Carcinoma with Different Sizes of Embolization Particles. *Dig. Dis. Sci.* **2008**, *53*, 1400–1404. [CrossRef] [PubMed]

68. Lee, K.-H.; Liapi, E.; Vossen, J.A.; Buijs, M.; Ventura, V.P.; Georgiades, C.; Hong, K.; Kamel, I.; Torbenson, M.S.; Geschwind, J.F. Distribution of Iron Oxide–containing Embosphere Particles after Transcatheter Arterial Embolization in an Animal Model of Liver Cancer: Evaluation with MR Imaging and Implication for Therapy. *J. Vasc. Interv. Radiol.* **2008**, *19*, 1490–1496. [CrossRef] [PubMed]

69. Wang, Z.-Y.; Song, J.; Zhang, D.-S. Nanosized As_2O_3/Fe_2O_3 complexes combined with magnetic fluid hyperthermia selectively target liver cancer cells. *World J. Gastroenterol.* **2009**, *15*, 2995–3002. [CrossRef] [PubMed]

70. Slowing, I.I.; Vivero-Escoto, J.L.; Wu, C.W.; Lin, V.S. Mesoporous silica nanoparticles as controlled release drug delivery and gene transfection carriers. *Adv. Drug Deliv. Rev.* **2008**, *60*, 1278–1288. [CrossRef] [PubMed]

71. Gu, J.; Su, S.; Li, Y.; He, Q.; Shi, J. Hydrophilic mesoporous carbon nanoparticles as carriers for sustained release of hydrophobic anti-cancer drugs. *Chem. Commun.* **2011**, *47*, 2101–2103. [CrossRef] [PubMed]

72. Stöber, W.; Fink, A.; Bohn, E. Controlled growth of monodisperse silica spheres in the micron size range. *J. Colloid Interface Sci.* **1968**, *26*, 62–69. [CrossRef]

73. Liu, J.; Qiao, S.Z.; Liu, H.; Chen, J.; Orpe, A.; Zhao, D.; Qing, G. Extension of the Stöber Method to the preparation of monodisperse resorcinol–formaldehyde resin polymer and carbon spheres. *Angew. Chem. Int. Ed.* **2011**, *50*, 5947–5951. [CrossRef] [PubMed]

74. Carroll, N.J.; Rathod, S.B.; Derbins, E.; Mendez, S.; Weitz, D.A.; Petsev, D.N. Droplet-based microfluidics for emulsion and solvent evaporation synthesis of monodisperse mesoporous silica microspheres. *Langmuir* **2008**, *24*, 658–661. [CrossRef] [PubMed]

75. Rao, G.V.R.; López, G.P.; Bravo, J.; Pham, H.; Datye, A.K.; Xu, H.F.; Ward, T.L. Monodisperse Mesoporous Silica Microspheres Formed by Evaporation-Induced Self Assembly of Surfactant Templates in Aerosols. *Adv. Mater.* **2002**, *14*, 1301–1304.

76. Song, H.; Tice, J.D.; Ismagilov, R.F. A Microfluidic System for Controlling Reaction Networks in Time. *Angew. Chem. Int. Ed.* **2003**, *42*, 768–772. [CrossRef] [PubMed]

77. Habault, D.; Dery, A.; Leng, J.; Lecommandoux, S.; Le Meins, J.F.; Sandre, O. Droplet Microfluidics to Prepare Magnetic Polymer Vesicles and to Confine the Heat in Magnetic Hyperthermia. *IEEE Trans. Magn.* **2013**, *49*, 182–190. [CrossRef]

78. Zhang, J.; Coulston, R.J.; Jones, S.T.; Geng, J.; Scherman, O.A.; Abell, C. One-Step Fabrication of Supramolecular Microcapsules from Microfluidic Droplets. *Science* **2012**, *335*, 690–694. [CrossRef] [PubMed]

79. Zhao, C.-X.; He, L.; Qiao, S.Z.; Middelberg, A.P. Nanoparticle synthesis in microreactors. *Chem. Eng. Sci.* **2011**, *66*, 1463–1479. [CrossRef]

80. Chen, C.-H.; Shah, R.K.; Abate, A.R.; Weitz, D.A. Janus particles templated from double emulsion droplets generated using microfluidics. *Langmuir* **2009**, *25*, 4320–4323. [CrossRef] [PubMed]

81. Song, Y.; Modrow, H.; Henry, L.L.; Saw, C.K.; Doomes, E.; Palshin, V.; Hormes, J.; Kumar, C.S.S.R. Microfluidic synthesis of cobalt nanoparticles. *Chem. Mater.* **2006**, *18*, 2817–2827. [CrossRef]

82. Wagner, J.; Köhler, J.M. Continuous Synthesis of Gold Nanoparticles in a Microreactor. *Nano Lett.* **2005**, *5*, 685–691. [CrossRef] [PubMed]

83. Hler, J.M.; Romanus, H.; Bner, U.; Wagner, J. Formation of Star-Like and Core-Shell AuAg Nanoparticles during Two- and Three-Step Preparation in Batch and in Microfluidic Systems. *J. Nanomater.* **2007**, *2007*, 98134.

84. Köhler, J.M.; Held, M.; Hübner, U.; Wagner, J. Formation of Au/Ag Nanoparticles in a Two Step Micro Flow-Through Process. *Chem. Eng. Technol.* **2007**, *30*, 347–354. [CrossRef]

85. Duraiswamy, S.; Khan, S.A. Droplet-Based Microfluidic Synthesis of Anisotropic Metal Nanocrystals. *Small* **2009**, *5*, 2828–2834. [CrossRef] [PubMed]

86. Wei, X.; Kong, T.; Wang, L. Copper Nanoparticles and Nanofluids-based W/O Emulsions Synthesized with Droplet Microreactors. *Curr. Nanosci.* **2012**, *8*, 117–119. [CrossRef]

87. Chan, E.M.; Alivisatos, A.P.; Mathies, R.A. High-temperature microfluidic synthesis of CdSe nanocrystals in nanoliter droplets. *J. Am. Chem. Soc.* **2005**, *127*, 13854–13861. [CrossRef] [PubMed]

88. Tice, J.D.; Lyon, A.D.; Ismagilov, R.F. Effects of viscosity on droplet formation and mixing in microfluidic channels. *Anal. Chim. Acta* **2004**, *507*, 73–77. [CrossRef]

89. Bentley, B.J.; Leal, L.G. An experimental investigation of drop deformation and breakup in steady, two-dimensional linear flows. *J. Fluid Mech.* **1986**, *167*, 241–283. [CrossRef]

90. Kong, T.; Liu, Z.; Song, Y.; Wang, L.; Shum, H.C. Engineering polymeric composite particles by emulsion-templating: Thermodynamics versus kinetics. *Soft Matter.* **2013**, *9*, 9780–9784. [CrossRef]

91. Lu, Y.; Yin, Y.; Xia, Y. Three-Dimensional Photonic Crystals with Non-spherical Colloids as Building Blocks. *Adv. Mater.* **2001**, *13*, 415–420. [CrossRef]

92. Langer, R.; Tirrell, D.A. Designing materials for biology and medicine. *Nature* **2004**, *428*, 487–492. [CrossRef] [PubMed]

93. Bonderer, L.J.; Studart, A.R.; Gauckler, L.J. Bioinspired design and assembly of platelet reinforced polymer films. *Science* **2008**, *319*, 1069–1073. [CrossRef] [PubMed]

94. Liu, Z.; Cai, W.; He, L.; Nakayama, N.; Chen, K.; Sun, X.; Chen, X.; Dai, H. In vivo biodistribution and highly efficient tumour targeting of carbon nanotubes in mice. *Nat. Nanotechnol.* **2007**, *2*, 47–52. [CrossRef] [PubMed]

95. Shum, H.C.; Abate, A.R.; Lee, D.; Studart, A.R.; Wang, B.; Chen, C.H.; Thiele, J.; Shah, R.K.; Krummel, A.; Weitz, D.A. Droplet Microfluidics for Fabrication of Non-Spherical Particles. *Macromol. Rapid Commun.* **2010**, *31*, 108–118. [CrossRef] [PubMed]

96. Haghgooie, R.; Toner, M.; Doyle, P.S. Squishy Non-Spherical Hydrogel Microparticles. *Macromol. Rapid Commun.* **2010**, *31*, 128–134. [CrossRef] [PubMed]

97. Subramaniam, A.B.; Abkarian, M.; Mahadevan, L.; Stone, H.A. Colloid science: Non-spherical bubbles. *Nature* **2005**, *438*, 930. [CrossRef] [PubMed]

98. Nie, Z.; Xu, S.; Seo, M.; Lewis, P.C.; Kumacheva, E. Polymer particles with various shapes and morphologies produced in continuous microfluidic reactors. *J. Am. Chem. Soc.* **2005**, *127*, 8058–8063. [CrossRef] [PubMed]

99. Rolland, J.P.; Maynor, B.W.; Euliss, L.E.; Exner, A.E.; Denison, G.M.; DeSimone, J.M. Direct fabrication and harvesting of monodisperse, shape-specific nanobiomaterials. *J. Am. Chem. Soc.* **2005**, *127*, 10096–10100. [CrossRef] [PubMed]

100. Kim, J.W.; Larsen, R.J.; Weitz, D.A. Uniform nonspherical colloidal particles with tunable shapes. *Adv. Mater.* **2007**, *19*, 2005–2009. [CrossRef]

101. Sacanna, S.; Pine, D.J. Shape-anisotropic colloids: Building blocks for complex assemblies. *Curr. Opin. Colloid Interface Sci.* **2011**, *16*, 96–105. [CrossRef]

102. Dendukuri, D.; Tsoi, K.; Hatton, T.A.; Doyle, P.S. Controlled Synthesis of Nonspherical Microparticles Using Microfluidics. *Langmuir* **2005**, *21*, 2113–2116. [CrossRef] [PubMed]

103. Dendukuri, D.; Pregibon, D.C.; Collins, J.; Hatton, T.A.; Doyle, P.S. Continuous-flow lithography for high-throughput microparticle synthesis. *Nat. Mater.* **2006**, *5*, 365–369. [CrossRef] [PubMed]

104. Yang, J.; Lind, J.U.; Trogler, W.C. Synthesis of hollow silica and titania nanospheres. *Chem. Mater.* **2008**, *20*, 2875–2877. [CrossRef]

105. Wu, D.; Ge, X.; Zhang, Z.; Wang, M.; Zhang, S. Novel one-step route for synthesizing CdS/polystyrene nanocomposite hollow spheres. *Langmuir* **2004**, *20*, 5192–5195. [CrossRef] [PubMed]

106. Wang, X.; Feng, J.; Bai, Y.; Zhang, Q.; Yin, Y. Synthesis, Properties, and Applications of Hollow Micro-/Nanostructures. *Chem. Rev.* **2016**, *116*, 10983–11060. [CrossRef] [PubMed]

107. Wang, W.; Zhang, M.J.; Xie, R.; Ju, X.J.; Yang, C.; Mou, C.L.; Weitz, D.A.; Chu, L.Y. Hole–Shell Microparticles from Controllably Evolved Double Emulsions. *Angew. Chem. Int. Ed.* **2013**, *52*, 8084–8087. [CrossRef] [PubMed]

108. Khan, I.U.; Serra, C.A.; Anton, N.; Vandamme, T. Continuous-flow encapsulation of ketoprofen in copolymer microbeads via co-axial microfluidic device: Influence of operating and material parameters on drug carrier properties. *Int. J. Pharm.* **2013**, *441*, 809–817. [CrossRef] [PubMed]

109. Utada, A.; Chu, L.-Y.; Fernandez-Nieves, A.; Link, D.; Holtze, C.; Weitz, D. Dripping, jetting, drops, and wetting: The magic of microfluidics. *MRS Bull.* **2007**, *32*, 702–708. [CrossRef]

110. Kim, J.W.; Utada, A.S.; Hu, Z.; Weitz, D.A. Fabrication of monodisperse gel shells and functional microgels in microfluidic devices. *Angew. Chem. Int. Ed.* **2007**, *46*, 1819–1822. [CrossRef] [PubMed]

111. Tomotika, S. Breaking up of a drop of viscous liquid immersed in another viscous fluid which is extending at a uniform rate. *Proc. R. Soc. Lond. Ser. A Math. Phys. Sci.* **1936**, *153*, 302–318. [CrossRef]

112. Chang, Z.; Serra, C.A.; Bouquey, M.; Prat, L.; Hadziioannou, G. Co-axial capillaries microfluidic device for synthesizing size- and morphology-controlled polymer core-polymer shell particles. *Lab Chip* **2009**, *9*, 3007–3011. [CrossRef] [PubMed]

113. Dowding, P.J.; Atkin, R.; Vincent, B.; Bouillot, P. Oil core-polymer shell microcapsules prepared by internal phase separation from emulsion droplets. I. Characterization and release rates for microcapsules with polystyrene shells. *Langmuir* **2004**, *20*, 11374–11379. [CrossRef] [PubMed]

114. Shum, H.C.; Kim, J.-W.; Weitz, D.A. Microfluidic fabrication of monodisperse biocompatible and biodegradable polymersomes with controlled permeability. *J. Am. Chem. Soc.* **2008**, *130*, 9543–9549. [CrossRef] [PubMed]

115. Guzowski, J.; Korczyk, P.M.; Jakiela, S.; Garstecki, P. The structure and stability of multiple micro-droplets. *Soft Matter* **2012**, *8*, 7269–7278. [CrossRef]

116. Loxley, A.; Vincent, B. Preparation of poly (methylmethacrylate) microcapsules with liquid cores. *J. Colloid Interface Sci.* **1998**, *208*, 49–62. [CrossRef] [PubMed]

117. Kim, J.H.; Jeon, T.Y.; Choi, T.M.; Shim, T.S.; Kim, S.-H.; Yang, S.-M. Droplet Microfluidics for Producing Functional Microparticles. *Langmuir* **2014**, *30*, 1473–1488. [CrossRef] [PubMed]

118. Perro, A.; Reculusa, S.; Ravaine, S.; Bourgeat-Lami, E.; Duguet, E. Design and synthesis of Janus micro-and nanoparticles. *J. Mater. Chem.* **2005**, *15*, 3745–3760. [CrossRef]

119. Schick, I.; Lorenz, S.; Gehrig, D.; Schilmann, A.-M.; Bauer, H.; Panthoefer, M.; Fischer, K.; Strand, D.; Laquai, F.; Tremel, W. Multifunctional Two-Photon Active Silica-Coated Au@ MnO Janus Particles for Selective Dual Functionalization and Imaging. *J. Am. Chem. Soc.* **2014**, *136*, 2473–2483. [CrossRef] [PubMed]

120. Walther, A.; Hoffmann, M.; Müller, A.H. Emulsion polymerization using Janus particles as stabilizers. *Angew. Chem.* **2008**, *120*, 723–726. [CrossRef]

121. Binks, B.; Fletcher, P. Particles adsorbed at the oil-water interface: A theoretical comparison between spheres of uniform wettability and "Janus" particles. *Langmuir* **2001**, *17*, 4708–4710. [CrossRef]

122. Gangwal, S.; Cayre, O.J.; Velev, O.D. Dielectrophoretic assembly of metallodielectric Janus particles in AC electric fields. *Langmuir* **2008**, *24*, 13312–13320. [CrossRef] [PubMed]

123. Khan, I.U.; Serra, C.A.; Anton, N.; Xiang, L.; Akasov, R.; Messaddeq, N.; Kraus, I.; Vandamme, T.F. Microfluidic conceived drug loaded Janus particles in side-by-side capillaries device. *Int. J. Pharm.* **2014**, *473*, 239–249. [CrossRef] [PubMed]

124. Shepherd, R.F.; Conrad, J.C.; Rhodes, S.K.; Link, D.R.; Marquez, M.; Weitz, D.A.; Lewis, J.A. Microfluidic assembly of homogeneous and janus colloid-filled hydrogel granules. *Langmuir* **2006**, *22*, 8618–8622. [CrossRef] [PubMed]

125. Seiffert, S.; Romanowsky, M.B.; Weitz, D.A. Janus microgels produced from functional precursor polymers. *Langmuir* **2010**, *26*, 14842–14847. [CrossRef] [PubMed]

126. Nie, Z.; Li, W.; Seo, M.; Xu, S.; Kumacheva, E. Janus and ternary particles generated by microfluidic synthesis: Design, synthesis, and self-assembly. *J. Am. Chem. Soc.* **2006**, *128*, 9408–9412. [CrossRef] [PubMed]

127. Dendukuri, D.; Hatton, T.A.; Doyle, P.S. Synthesis and self-assembly of amphiphilic polymeric microparticles. *Langmuir* **2007**, *23*, 4669–4674. [CrossRef] [PubMed]

128. Prasad, N.; Perumal, J.; Choi, C.H.; Lee, C.S.; Kim, D.P. Generation of monodisperse inorganic–organic Janus microspheres in a microfluidic device. *Adv. Funct. Mater.* **2009**, *19*, 1656–1662. [CrossRef]

129. Windbergs, M.; Zhao, Y.; Heyman, J.A.; Weitz, D.A. Biodegradable core-shell carriers for simultaneous encapsulation of synergistic actives. *J. Am. Chem. Soc.* **2013**. [CrossRef] [PubMed]

130. Sekhar, A.S.; Meera, C.; Ziyad, K.; Gopinath, C.S.; Vinod, C. Synthesis and catalytic activity of monodisperse gold–mesoporous silica core–shell nanocatalysts. *Catal. Sci. Technol.* **2013**, *3*, 1190–1193. [CrossRef]

131. DiLauro, A.M.; Abbaspourrad, A.; Weitz, D.A.; Phillips, S.T. Stimuli-Responsive Core–Shell Microcapsules with Tunable Rates of Release by Using a Depolymerizable Poly(phthalaldehyde) Membrane. *Macromolecules* **2013**, *46*, 3309–3313. [CrossRef]

132. Dawes, G.; Fratila-Apachitei, L.; Mulia, K.; Apachitei, I.; Witkamp, G.-J.; Duszczyk, J. Size effect of PLGA spheres on drug loading efficiency and release profiles. *J. Mater. Sci. Mater. Med.* **2009**, *20*, 1089–1094. [CrossRef] [PubMed]

133. Siepmann, J.; Faisant, N.; Akiki, J.; Richard, J.; Benoit, J. Effect of the size of biodegradable microparticles on drug release: Experiment and theory. *J. Control. Release* **2004**, *96*, 123–134. [CrossRef] [PubMed]

134. Lee, T.H.; Wang, J.; Wang, C.-H. Double-walled microspheres for the sustained release of a highly water soluble drug: Characterization and irradiation studies. *J. Control. Release* **2002**, *83*, 437–452. [CrossRef]

135. Berkland, C.; Cox, A.; Kim, K.K.; Pack, D.W. Three-month, zero-order piroxicam release from monodispersed double-walled microspheres of controlled shell thickness. *J. Biomed. Mater. Res. Part A* **2004**, *70*, 576–584. [CrossRef] [PubMed]

136. Chu, L.-Y.; Utada, A.S.; Shah, R.K.; Kim, J.-W.; Weitz, D.A. Controllable monodisperse multiple emulsions. *Angew. Chem. Int. Ed.* **2007**, *46*, 8970–8974. [CrossRef] [PubMed]

137. Sun, X.; Li, Y. Colloidal Carbon Spheres and Their Core/Shell Structures with Noble-Metal Nanoparticles. *Angew. Chem. Int. Ed.* **2004**, *43*, 597–601. [CrossRef] [PubMed]

138. Guo, S.R.; Gong, J.Y.; Jiang, P.; Wu, M.; Lu, Y.; Yu, S.H. Biocompatible, Luminescent Silver@ Phenol Formaldehyde Resin Core/Shell Nanospheres: Large-Scale Synthesis and Application for In Vivo Bioimaging. *Adv. Funct. Mater.* **2008**, *18*, 872–879. [CrossRef]

139. Fang, Y.; Gu, D.; Zou, Y.; Wu, Z.; Li, F.; Che, R.; Deng, Y.; Tu, B.; Zhao, D. A Low-Concentration Hydrothermal Synthesis of Biocompatible Ordered Mesoporous Carbon Nanospheres with Tunable and Uniform Size. *Angew. Chem. Int. Ed.* **2010**, *49*, 7987–7991. [CrossRef] [PubMed]

140. Guo, L.; Zhang, L.; Zhang, J.; Zhou, J.; He, Q.; Zeng, S.; Cui, X.; Shi, J. Hollow mesoporous carbon spheres—An excellent bilirubin adsorbent. *Chem. Commun.* **2009**, *40*, 6071–6073. [CrossRef] [PubMed]

141. Ju, M.; Zeng, C.; Wang, C.; Zhang, L. Preparation of ultrafine carbon spheres by controlled polymerization of furfuryl alcohol in microdroplets. *Ind. Eng. Chem. Res.* **2014**, *53*, 3084–3090. [CrossRef]

142. Pan, Y.; Ju, M.; Wang, C.; Zhang, L.; Xu, N. Versatile preparation of monodisperse poly (furfuryl alcohol) and carbon hollow spheres in a simple microfluidic device. *Chem. Commun.* **2010**, *46*, 3732–3734. [CrossRef] [PubMed]

143. Zhu, T.; Cheng, R.; Sheppard, G.R.; Locklin, J.; Mao, L. Magnetic-Field-Assisted Fabrication and Manipulation of Nonspherical Polymer Particles in Ferrofluid-Based Droplet Microfluidics. *Langmuir* **2015**, *31*, 8531–8534. [CrossRef] [PubMed]

144. Sánchez-Ferrer, A.; Carney, R.P.; Stellacci, F.; Mezzenga, R.; Isa, L. Isolation and Characterization of Monodisperse Core–Shell Nanoparticle Fractions. *Langmuir* **2015**, *31*, 11179–11185. [CrossRef] [PubMed]

145. Bermudez, H.; Brannan, A.K.; Hammer, D.A.; Bates, F.S.; Discher, D.E. Molecular weight dependence of polymersome membrane structure, elasticity, and stability. *Macromolecules* **2002**, *35*, 8203–8208. [CrossRef]

146. Lee, J.C.M.; Bermudez, H.; Discher, B.M.; Sheehan, M.A.; Won, Y.Y.; Bates, F.S.; Discher, D.E. Preparation, stability, and in vitro performance of vesicles made with diblock copolymers. *Biotechnol. Bioeng.* **2001**, *73*, 135–145. [CrossRef] [PubMed]

147. Aranda-Espinoza, H.; Bermudez, H.; Bates, F.S.; Discher, D.E. Electromechanical limits of polymersomes. *Phys. Rev. Lett.* **2001**, *87*, 208301. [CrossRef] [PubMed]

148. Wang, C.; Wang, L.; Wang, M. Evolution of core–shell structure: From emulsions to ultrafine emulsion electrospun fibers. *Mater. Lett.* **2014**, *124*, 192–196. [CrossRef]

149. Kong, T.; Wang, L.; Wyss, H.M.; Shum, H.C. Capillary micromechanics for core-shell particles. *Soft Matter* **2014**, *10*, 3271–3276. [CrossRef] [PubMed]